



Structure and X-ray conformation of pseudodesmins A and B, two new cyclic lipodepsipeptides from *Pseudomonas* bacteria

Davy Sinnaeve^{a,*}, Catherine Michaux^b, Johan Van hemel^c, Jan Vandankerckhove^c, Eric Peys^c, Frans A.M. Borremans^a, Benedikt Sas^{c,†}, Johan Wouters^b, José C. Martins^{a,*}

^aNMR and Structure Analysis Unit, Department of Organic Chemistry, Ghent University, Krijgslaan 281 S4, B-9000 Gent, Belgium

^bLaboratoire de Chimie Biologique Structurale, Université de Namur, rue de Bruxelles 61, B-5000 Namur, Belgium

^cKemin Pharma, Atealaan 4H, B-2200 Herentals, Belgium

ARTICLE INFO

Article history:

Received 9 February 2009

Received in revised form 11 March 2009

Accepted 16 March 2009

Available online 26 March 2009

Keywords:

Lipodepsipeptide
Viscosin group
Pseudodesmin
Pseudomonas
Plethodontidae
X-ray structure
NMR

ABSTRACT

Two new cyclic lipodepsipeptides named pseudodesmins A and B have been isolated from *Pseudomonas* bacteria collected from the mucus layer in the skin of the black belly salamander. Both compounds show moderate antibacterial activity against Gram positive bacteria, including MRSA. Complete ¹H, ¹³C and ¹⁵N NMR assignment of both compounds afforded their covalent structure and served to guide the analysis of LC–MS and X-ray diffraction data from which the final stereochemistry could be established. Both molecules can be categorized as new members of the viscosin group of cyclic lipodepsipeptides.

© 2009 Elsevier Ltd. All rights reserved.

1. Introduction

Cyclic lipodepsipeptides (CLPs) are secondary metabolites produced mainly by *Pseudomonas* bacteria,^{1,2} and are of interest as they display potential antimicrobial activity. They consist of an oligopeptide chain that forms a cyclic structure via a lactone (or so-called depsi) bond involving the C-terminus, and a long fatty acid chain that is connected to the exocyclic N-terminus. CLPs are believed to have several extracellular functions, including surface motility, biosurfactant activity and antimicrobial activity. Because CLPs are not bound to the rules of ribosomal synthesis,² uncommon or modified amino acids, including D-amino acids, are often present. They have been classified into several groups, including the viscosin group, the amphisin group, the syringomycin group and the tol-aasin group.^{1,2} With the exception of the latter, the peptide chain

length within each group is the same and a similar sequence distribution pattern in hydrophobic and hydrophilic residues can be observed. The viscosin group comprises viscosin,³ viscosinamide,⁴ White Line Inducing Principle (WLIP),⁵ massetolides A–H⁶ and pseudophomins A and B,⁷ which all consist of nine amino acid residues, seven of which form the cyclic structure via lactone bond formation between the C-terminus and the side chain of a D-allo-Thr at position 3. They are produced by several *Pseudomonas* species, including *P. viscosa*,⁸ *P. libanensis*⁹ (viscosin), different strains of *P. fluorescens* (viscosin,¹⁰ viscosinamide,⁴ the massetolides¹¹ and pseudophomins⁷) and *P. reactans* (WLIP⁵).

Here we report the isolation, biological activity and conformation of two new CLPs, pseudodesmins A and B (Fig. 1). They originate from *Pseudomonas* bacteria living in the mucus layer of salamanders of the *Plethodontidae* family and are shown to display moderate antibiotic activities. Full elucidation of the covalent structure was achieved through NMR, LC–MS and X-ray diffraction analysis, revealing pseudodesmins A and B to be new members of the viscosin group. For certain viscosin group members, transmembrane pore formation has been proposed as the most likely biological mode of action.^{12,13} Using the crystal structure of pseudodesmin A, potential links between the structure and this mode of action are discussed.

* Corresponding authors. Tel.: +32 (0)9 264 4469; fax: +32 (0)9 264 4972.

E-mail addresses: davy.sinnaeve@ugent.be (D. Sinnaeve), jose.martins@ugent.be (J.C. Martins).

† Present address: Department of Food Safety and Food Quality, Ghent University, Coupure Links 653, blok B, 9000 Gent, Belgium.

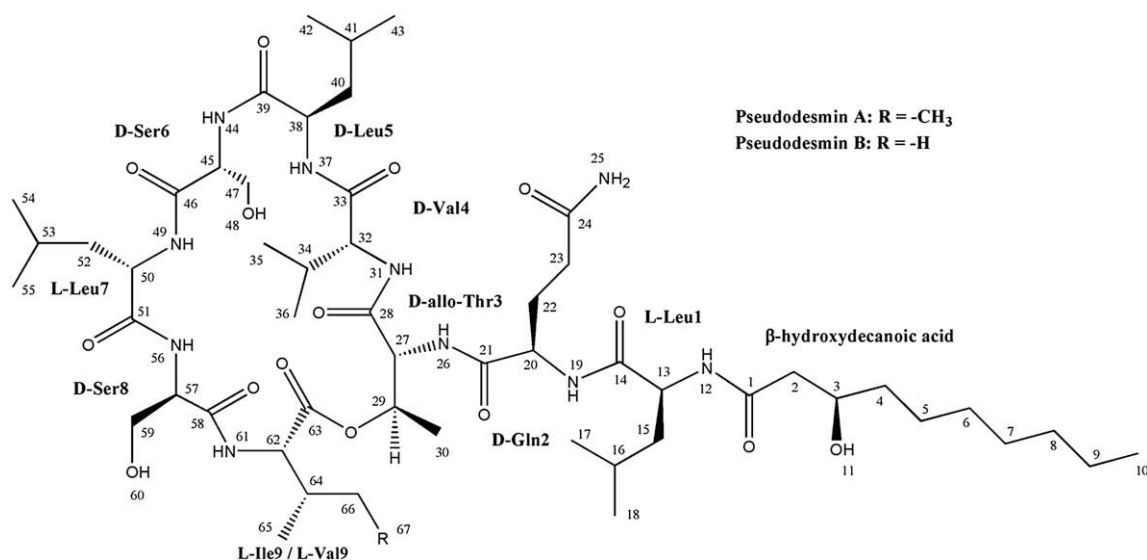


Figure 1. Molecular structure of pseudodesmins A and B.

2. Results

2.1. Pseudodesmins A and B display moderate antibacterial and antiviral activities

The newly isolated compounds were scrutinized for biological activity against a series of Tier one pathogens. The results of the antibiotic, antimycotic, antiviral and cytotoxic screenings are presented in Tables 1 and 2. Pseudodesmins A and B both possess bacteriostatic properties against Gram positive bacteria, including several resistant strains. However, no bacteriocidal effects were observed at concentrations up to 25 µg/ml (maximum test dosage). Only a modest antiviral activity against HIV1 and VZV and some cytostatic activity can be observed for the mixture of pseudodesmins A and B, whereas no significant antimycotic activity is observed.

2.2. Structure elucidation of pseudodesmins A and B

Initial LC–MS studies revealed the molecular weights of pseudodesmins A and B to be 1124.2 Da and 1110.2 Da, respectively.

Using MS/MS analysis data alone, no conclusive proposal for the molecular structure could be made, however, the presence of a cyclic oligopeptide fragment was already suspected. In addition, the absence of a free amino group was revealed from a negative response to a ninhydrine colouring test. The oligopeptide nature was confirmed using NMR spectroscopy. The 2D TOCSY spectrum showed correlations between amide resonances and aliphatic spin systems characteristic for amino acid moieties. Full assignment and structure confirmation was achieved in a 2 mM acetonitrile solution. Combined analysis of a 2D DQF-COSY and a ¹H–¹³C–HSQC spectrum revealed 10 separate spin systems for pseudodesmin A, corresponding to 9 amino acid residues (one Glx, three Leu's, one Thr, two Ser's, one Val and one Ile) and a 2-hydroxyonyl (R) spin system. The sequence of these residues was established through a 200 ms NOESY spectrum from sequential H^α to H^N NOE's, including a connection between the αCH₂ of the 2-hydroxyonyl moiety and the H^N of Leu1. In addition, NOE contacts between the γ protons of the Glx spin system to two resonances in the amide region of the spectrum that exclusively correlate with each other in COSY and TOCSY spectra, established the Glx residue as a Gln. The primary structure of pseudodesmin A was thus established as R-Leu-Gln-Thr-Val-Leu-

Table 1
Antibacterial and antifungal activity

Compound	MIC (µg/ml)					
	<i>E. faecalis</i> ATCC 29212 LMG 8222	VRE ATCC 700221	<i>S. aureus</i> ATCC 29213 LMG 10147	MRSA ATCC 33591 LMG 16217	<i>P. aeruginosa</i> ATCC 27853 LMG 6395	<i>S. typhimurium</i> ATCC 700408 LMG 16217
Pseudodesmin A	3.12–6.25	3.12–6.25	3.12–6.25	6.25–12.5	>25	>25
Pseudodesmin B	6.25–12.5	3.12–6.25	6.25–12.5	6.25–12.5	>25	>25
Positive control	1.0–2.5 ^a	>10 ^a	0.1–0.5 ^a	0.5–1.0 ^a	0.1–0.5 ^b	0.1–0.5 ^b
Compound	MIC (µg/ml)					
	<i>E. coli</i> ATCC 25922	<i>C. perfringens</i> ATCC 13124	<i>C. albicans</i> IHEM 10248 ATCC 24433	<i>C. neoformans</i> IHEM 9558 ATCC 90112	<i>T. mentagrophytes</i> IHEM 10342 ATCC 9533	
Pseudodesmin A	>25	3.12–6.25	>25	>25	>25	
Pseudodesmin B	>25	3.12–6.25	>25	>25	>25	
Positive control	0.1–0.5 ^b	0.25–0.5 ^a	0.75 ^c	0.75 ^c	5 ^c	

The lower value is the highest concentration where inhibition was detected, the higher value is the lowest concentration where no inhibition was detected. The maximum concentration tested was 25 µg/ml. MIC values of positive control compounds were determined in parallel.

^a Vancomycin.

^b Gentamycin.

^c Amphotericin B.

Table 2
Antiviral activity and cytotoxic activity

Compound	EC ₅₀ (μg/ml)						
	HIV-1 (III _B) (CEM)	HIV-2 (ROD) (CEM)	HSV-1 (KOS) (E ₆ SM)	HSV-2 (G) (E ₆ SM)	VV (E ₆ SM)	VZV (HEL) OKA YS	
Pseudodesmins A+B	7.3	17.3	>16	>16	>16	3	3
Reference value	0.0063 ^a	0.0097 ^a	0.07 ^b	0.38 ^b	3.2 ^c	0.24 ^b	0.32 ^b
Compound	IC ₅₀ (μg/ml)						
	CMV		L1210/0	FM3A/0	Molt4/C8	CEM/0	
	AD-169 strain	Davis strain					
Pseudodesmins A+B	8	>5	17	16	17	17	
Reference value	1.2 ^d	0.6 ^d	—	—	—	—	

Reference values of standard compounds are provided for comparison.²³^a AZT.^b Acyclovir.^c Brivudin.^d Ganciclovir.

Ser-Leu-Ser-Ile. Finally, the ¹H–¹³C gHMBC allowed to assign all the carbonyl ¹³C resonances through ²J_{CH} coupling correlations with the H^N or H^α resonances. The 2-hydroxyonyl spin system could be assigned to a 3-hydroxydecanoic acid (HDA) moiety. Most importantly, a clear ³J_{CH} correlation between the Thr3 H^β and the Ile9 carbonyl resonances unambiguously demonstrated the presence of a lactone bond, revealing a cyclic heptapeptide structure with two exocyclic residues at the N-terminus. The final covalent structure thus derived (Fig. 1) was in agreement with the molecular weight previously determined by LC–MS. Finally, ¹⁵N assignments were established at natural abundance via a 2D ¹H–¹⁵N gHSQC at 700 MHz. Structure elucidation and NMR assignment of pseudodesmin B were obtained in a similar fashion and revealed the substitution of the Ile9 residue for a second Val residue as the only difference with pseudodesmin A, in accordance with the 14 Da mass difference. The complete assignments of both molecules are collected in Tables 3 and 4, while 1D ¹H and 2D HSQC spectra are provided in Supplementary data.

To establish the stereochemistry, pseudodesmin A was subjected to total hydrolysis followed by derivatization of the free amino acids with Marfey's reagent¹⁴ and LC–MS analysis. The presence of two L-Leu, one D-Leu, two D-Ser, one D-allo-Thr, one D-Val and one L-Ile could be established. After lengthy crystallization trials, a crystal structure of pseudodesmin A was obtained from acetonitrile solution, which finally revealed the absolute configuration of the remaining stereocentres ((3R)-HDA, D-Gln2 and the D-Leu at position 5), the LC–MS being critical to distinguish between

Table 3
¹H, ¹³C and ¹⁵N NMR assignments of pseudodesmin A (CD₃CN, 298 K, 700 MHz)

		¹ H δ [ppm]	¹³ C δ [ppm]	¹⁵ N δ [ppm]			¹ H δ [ppm]	¹³ C δ [ppm]	¹⁵ N δ [ppm]			
HDA	Leu5 ³ J _{HNHα}	CO 1	175.27		Leu5 ³ J _{HNHα}	4.25 Hz	NH 37	7.72	–266.48			
		CH ₂ α 2	2.34/2.43	44.81		CHα 38	3.97	55.74				
		CHβ 3	3.97	69.53		CO 39		173.62				
		CH ₂ γ 4	1.47	38.27		CH ₂ β 40	1.51/1.66	40.71				
		CH ₂ δ 5	1.31/1.41	26.36		CHγ 41	1.77	25.53				
		CH ₂ ε 6	1.29	30.20		CH ₃ δ 42	0.87	23.36				
		CH ₂ ζ 7	1.29	30.20		CH ₃ δ 43	0.88	21.34				
		CH ₂ η 8	1.27	32.63		Ser6 ³ J _{HNHα}	8.47 Hz	NH 44		7.11	–276.91	
		CH ₂ θ 9	1.29	23.44				CHα 45		4.32		56.45
		CH ₃ 10	0.88	14.44				CO 46				171.93
		Leu1 ³ J _{HNHα}	5.67 Hz	OH 11		4.40	Leu7 ³ J _{HNHα}	6.53 Hz		CH ₂ β 47	3.81/4.15	64.80
NH 12	7.73				OHγ 48	4.98						
CHα 13	3.87			53.92	NH 49	7.10						
CO 14				175.34	CHα 50	4.13			54.90			
CH ₂ β 15	1.65/1.74			39.46	CO 51				173.80			
CHγ 16	1.67			25.46	CH ₂ β 52	1.58/1.88			42.11			
CH ₃ δ 17	0.90			22.16	CHγ 53	1.89			25.55			
Gln2 ³ J _{HNHα}	3.99 Hz	CH ₃ δ 18	0.94	23.21	CH ₃ δ 54	0.90	21.42	–273.98				
		NH 19	8.76		CH ₃ δ 55	0.99	23.53					
		CHα 20	3.98	57.58	Ser8 ³ J _{HNHα}	9.10 Hz	NH 56		7.94	–273.98		
		CO 21		176.63			CHα 57		4.43		57.02	
		CH ₂ β 22	2.02	26.35			CO 58				171.86	
		CH ₂ γ 23	2.38	32.01	CH ₂ β 59	3.66/3.86	63.25					
COδ 24		176.15	OHγ 60	3.80								
Thr3 ³ J _{HNHα} ³ J _{HαHβ}	7.45 Hz 10.71 Hz	NH ₂ 25	5.81/6.36		Ile9 ³ J _{HNHα}	10.70 Hz	NH 61	6.68	–270.70			
		NH 26	8.15				CHα 62	4.56		57.17		
		CHα 27	3.99	61.77			CO 63			170.12		
		CO 28		174.33			CHβ 64	1.97		36.97		
		CHβ 29	5.33	70.33			CH ₃ γ 65	0.82		16.28		
Val4 ³ J _{HNHα}	6.30 Hz	CH ₃ γ 30	1.30	18.58	CH ₂ γ 66	0.97/1.15	25.31	–259.73				
		NH 31	7.33		CH ₃ δ 67	0.86	12.36					
		CHα 32	3.49	65.08								
		CO 33		174.63								
		CHβ 34	2.17	30.02								
		CH ₃ γ 35	0.92	19.56								
CH ₃ γ 36	0.95	21.12										

Table 4
 ^1H , ^{13}C and ^{15}N NMR assignments of pseudodesmin B (CD_3CN , 298 K, 700 MHz)

		^1H δ [ppm]	^{13}C δ [ppm]	^{15}N δ [ppm]			^1H δ [ppm]	^{13}C δ [ppm]	^{15}N δ [ppm]
HDA					Leu5 $^3J_{\text{HNH}\alpha}$	3.99 Hz	NH 37 CH α 38 CO 39	7.77 3.97 173.68	
		CO 1	175.14				CH $_2\beta$ 40 CH γ 41	1.50/1.67 1.77	
		CH $_2\alpha$ 2	44.76				CH $_3\delta$ 42 CH $_3\delta$ 43	0.86 0.87	
		CH β 3	69.64		Ser6 $^3J_{\text{HNH}\alpha}$	8.33 Hz	NH 44 CH α 45 CO 46	7.14 4.32 172.03	-276.70
		CH $_2\gamma$ 4	38.29				CH $_2\beta$ 47 OH γ 48	3.81/4.15 4.99	
		CH $_2\delta$ 5	26.36		Leu7 $^3J_{\text{HNH}\alpha}$	6.23 Hz	NH 49 CH α 50 CO 51	7.11 4.14 173.88	-260.54
		CH $_2\epsilon$ 6	30.12				CH $_2\beta$ 52 CH γ 53	1.61/1.89 1.88	
		CH $_2\zeta$ 7	30.12				CH $_3\delta$ 54 CH $_3\delta$ 55	0.90 0.98	
		CH $_2\eta$ 8	32.59		Ser8 $^3J_{\text{HNH}\alpha}$	8.96 Hz	NH 56 CH α 57 CO 58	7.95 4.44 172.02	-273.86
		CH $_2\theta$ 9	23.44				CH $_2\beta$ 59 OH γ 60	3.66/3.86 3.83	
		CH $_3\iota$ 10	14.43		Val9 $^3J_{\text{HNH}\alpha}$	10.01 Hz	NH 61 CH α 62 CO 63	6.71 4.52 170.15	-271.43
		OH 11	3.65				CH β 64 CH $_3\gamma$ 65 CH $_2\gamma$ 66	2.23 0.72 19.49	
Leu1 $^3J_{\text{HNH}\alpha}$	ND	NH 12	7.94	-253.49			CH α 66	57.07	
		CH α 13	3.89				CO 67	173.88	
		CO 14					CH β 68	41.90	
		CH $_2\beta$ 15	1.66/1.74				CH γ 69	25.56	
		CH γ 16	1.67				CH $_3\delta$ 70	21.45	
		CH $_3\delta$ 17	0.90				CH $_3\delta$ 71	23.42	
		CH $_3\delta$ 18	0.93						
Gln2 $^3J_{\text{HNH}\alpha}$	ND	NH 19	8.78	-260.95					
		CH α 20	3.97						
		CO 21							
		CH $_2\beta$ 22	2.01						
		CH $_2\gamma$ 23	2.37						
		CO δ 24							
		NH $_2$ 25	5.82/6.42	-275.49					
Thr3 $^3J_{\text{HNH}\alpha}$ $^3J_{\text{H}\alpha\text{H}\beta}$	7.14 Hz 10.68 Hz	NH 26	8.20	-266.14					
		CH α 27	3.99						
		CO 28							
		CH β 29	5.33						
		CH $_3\gamma$ 30	1.30						
Val4 $^3J_{\text{HNH}\alpha}$	6.23 Hz	NH 31	7.41	-259.52					
		CH α 32	3.48						
		CO 33							
		CH β 34	2.16						
		CH $_3\gamma$ 35	0.90						
		CH $_3\gamma$ 36	0.95						

ND: not determined.

both possible enantiomers of the crystal structure. Due to limited material, pseudodesmin B was not subjected to total hydrolysis for chromatographic analysis and crystallization trials remained unsuccessful. However, except for the Ile/Val substitution, no significant differences in chemical shifts and $^3J_{\text{HNH}\alpha}$ scalar couplings between pseudodesmins A and B can be observed. Therefore, we are confident that the stereochemistry is identical, since one or multiple inversions of a single stereocentre would undoubtedly have a strong impact on the overall conformation and thus on the aforementioned conformation sensitive NMR parameters.

Both products were subjected to high resolution mass spectrometry analysis, of which the experimental details and full results are described in Supplementary data. This was performed at the Research Institute of Chromatography in Kortrijk, Belgium. The analysis provided a molecular weight of the protonated ion $[\text{M}+\text{H}]^+$ of 1125.71396 Da for pseudodesmin A and 1111.70019 Da for pseudodesmin B, which is in good agreement with the respective molecular formulas of $\text{C}_{54}\text{H}_{96}\text{N}_{10}\text{O}_{15}$ and $\text{C}_{53}\text{H}_{94}\text{N}_{10}\text{O}_{15}$.

2.3. The crystal structure of pseudodesmin A

The crystal structure of pseudodesmin A is presented in Figure 2, while general crystallographic parameters are provided in Table 5. Crystallographic data (excluding structure factors) have been deposited with the Cambridge Crystallographic Data Centre as supplementary publication CCDC 685601. Copies of the data can be obtained, free of charge, on application to CCDC, 12 Union Road,

Cambridge CB2 1EZ, UK, (fax: +44 (0)1223 336033 or e-mail: deposit@ccdc.cam.ac.uk). Based on the ϕ/ψ angles collected in Table 6, the conformation mainly consists of a short left-handed α -helix ranging from D-Gln2 to D-Leu5. The helix is stabilized by two $i+4 \rightarrow i$ hydrogen bonds (Leu5 NH \rightarrow Leu1 CO and Ser6 NH \rightarrow Gln2 CO) (Table 7) and is preceded by a type II β turn over the L-Leu1–D-Gln2

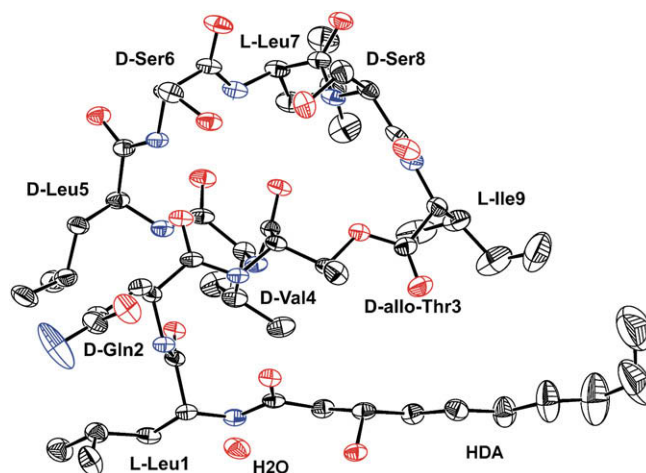


Figure 2. Crystal structure of pseudodesmin A with ellipsoids representing the B-factors.

Table 5
Crystallographic parameters for pseudodesmin A

Crystal data	
Space group	Orthorhombic, $P2_12_12_1$
Unit-cell parameters (Å)	$a=14.174(1)$, $b=18.796(1)$, $c=24.423(2)$
V	$6506.6(8) \text{ \AA}^3$
Z	4
m	0.71 mm^{-1}
Crystal size	$0.25 \times 0.20 \times 0.10 \text{ mm}$
Data collection	
Measured reflections	15,350
Independent reflections	8283
Reflections with $I > 2\sigma(I)$	6185
R_{int}	0.04
Refinement	
R	0.045
Reflections	8283
Parameters	737
DR_{max}	0.39 e \AA^{-3}
DR_{min}	-0.24 e \AA^{-3}

dipeptide and followed by a type I' β -turn over D -Leu5– D -Ser6. Both are accompanied by the characteristic hydrogen bonds, involving the NH of Thr3 with the CO of the HDA moiety and the NH of Leu7 and the CO of Val4, respectively. The switch to the L -configuration at Leu7 ends the α_L -helix, the main chain veering away right-handedly. The alternating L – D – L configuration in the Leu7–Ile9 tripeptide allows the backbone to loop back and brings the carboxylic end of the main chain in an adequate position to form the lactone bond with the Thr3 side chain (Fig. 3). The loop thus locks the N- and C-terminal ends of the α_L -helix together. It also caps the Thr3 and Val4 CO's by forming additional hydrogen bonds with the Ser8 NH and Leu7 NH, respectively. The Ile9 NH is not involved in any intramolecular hydrogen bond. All intramolecular and further intermolecular hydrogen bonds are listed in Table 7. Some of the intermolecular hydrogen bonds involve a single water molecule that acts as a hydrogen bond mediator between the C-terminal end of one molecule, where it caps the free carbonyl groups of Ser6 and Leu7, and the N-terminal end of the next one, where it interacts with the amide of Leu1.

The organization of the individual molecules is such that the hydrophobic side chains are packed together, delimiting large empty spaces between different units. The long alkyl chain of the HDA extends out into these spaces, where the high B-factors at the end of this chain are indicative of a higher degree of motional freedom.

3. Discussion

3.1. Biological activity of the pseudodesmins and comparison with the viscosin group

The current need for new lead compounds and antibiotic agents that circumvent the increasing levels of resistance against antibacterial and antiviral agents remains an important motivation in the search for new natural products with relevant biological activity. Pseudodesmins A and B are both mainly active against Gram positive bacteria such as VRE and MRSA. However, they are generally less potent and their inhibition spectrum is not as broad as standard antibiotics such as vancomycin. They also do not possess

Table 6
 ϕ and ψ Torsion angles of pseudodesmin A crystal structure

	Leu1	Gln2	Thr3	Val4	Leu5	Ser6	Leu7	Ser8	Ile9
ϕ [°]	–60.9	57.1	63.3	61.8	63.1	98.1	–66.4	150.7	–66.0
ψ [°]	122.7	28.5	40.5	48.6	31.7	1.0	–50.6	–41.2	–6.3

Table 7
Overview of pseudodesmin A hydrogen bonds

Intramolecular			
Donor	Acceptor	$d(D-A)$ [Å]	Angle [°]
Thr3 NH	HDA CO	2.95	152.05
Leu5 NH	Leu1 CO	3.15	165.35
Ser6 NH	Gln2 CO	2.82	149.16
Leu7 NH	Val4 CO	3.18	151.21
Ser8 NH	Thr3 CO	2.92	168.02
Intermolecular			
Participants		$d(D-A)$ [Å]	Angle [°]
HDA OH	Ser6 OH ^a	2.85	—
HDA CO	Ser8 OH ^a	2.79	160.87
Leu1 NH	H ₂ O ^b	2.83	164.69
Gln2 NH	Ser8 CO ^a	2.85	164.38
Val4 CO	Gln2 CONH ₂ ^c	2.78	168.51
Leu5 CO	Ile9 NH ^d	2.93	139.53
Ser6 CO	H ₂ O ^e	2.77	165.73
Leu7 CO	H ₂ O ^e	2.81	151.60

Hydrogen bonds are considered to have a donor–acceptor bond length of at least 3.4 Å and a bond angle of at least 140°.

^a Second participant coordinates are $(x-1/2, 3/2-y, 1-z)$.

^b Second participant coordinates are (x, y, z) .

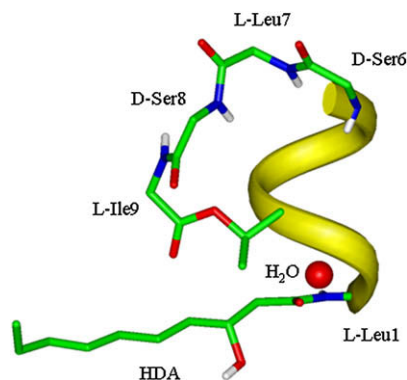
^c Second participant coordinates are $(1/2-x, 1-y, z-1/2)$.

^d Second participant coordinates are $(1-x, y+1/2, 1/2-z)$.

^e Second participant coordinates are $(x+1, y, z)$.

any noteworthy antifungal, antiviral or cytostatic activity. Pseudodesmins A and B are very similar to a collection of CLPs known as the viscosin group¹ (Fig. 4). A prominent distinction with all but one (viscosinamide) of the other members in this group is that they have a glutamine rather than a glutamic acid at position 2. It can be noted that pseudodesmin A differs from WLIP only by this D -Glu/ D -Gln substitution. Pseudodesmin A can thus be considered as WLIP-amide. Compared to viscosinamide, it only differs with respect to the stereochemistry of the Leu at position 5, being D rather than L . With an L -Val at position 9 pseudodesmin B differs by at least two substitutions from any previously known viscosin group member: WLIP (Ile9 and Glu2) and viscosinamide (L -Leu5 and Ile9). Only one other member, massetolide E, features an L -Val9, however, it has an L -Leu rather than a D -Leu at position 5 and a D -Glu instead of D -Gln.

Viscosin has been described by Kochi et al.⁸ to have no effect against most of the Gram positive and Gram negative bacteria that they tested. Later, both viscosin and the massetolides were reported to possess significant activity against *Mycobacterium tuberculosis* and *Mycobacterium avium-intracellulare*, but not against *Escherichia coli* and *Staphylococcus aureus*.⁶ The latter is a significant difference with the pseudodesmins, which could

**Figure 3.** Representation of the crystal structure of pseudodesmin A showing only the backbone atoms. The helix is shown as a ribbon (N→C from bottom to top), while the Leu7–Ile9 loop can be seen making the connection between the helix C-terminal and the Thr3 side chain.

Viscosin group

		1	2	3	4	5	6	7	8	9
pseudodesmin A	$\text{CH}_3(\text{CH}_2)_6\text{CH}(\text{OH})\text{CH}_2\text{CO}$	L-Leu	D-Gln	D-aThr	D--Val	D-Leu	D-Ser	L-Leu	D-Ser	L-Ile
pseudodesmin B	$\text{CH}_3(\text{CH}_2)_6\text{CH}(\text{OH})\text{CH}_2\text{CO}$	L-Leu	D-Gln	D-aThr	D--Val	D-Leu	D-Ser	L-Leu	D-Ser	L-Val
WLIP	$\text{CH}_3(\text{CH}_2)_6\text{CH}(\text{OH})\text{CH}_2\text{CO}$	L-Leu	D-Glu	D-aThr	D--Val	D-Leu	D-Ser	L-Leu	D-Ser	L-Ile
pseudophomin A	$\text{CH}_3(\text{CH}_2)_6\text{CH}(\text{OH})\text{CH}_2\text{CO}$	L-Leu	D-Glu	D-aThr	D--Ile	D-Leu	D-Ser	L-Leu	D-Ser	L-Ile
pseudophomin B	$\text{CH}_3(\text{CH}_2)_6\text{CH}(\text{OH})\text{CH}_2\text{CO}$	L-Leu	D-Glu	D-aThr	D--Ile	D-Leu	D-Ser	L-Leu	D-Ser	L-Ile
viscosin	$\text{CH}_3(\text{CH}_2)_6\text{CH}(\text{OH})\text{CH}_2\text{CO}$	L-Leu	D-Glu	D-aThr	D--Val	L-Leu	D-Ser	L-Leu	D-Ser	L-Ile
viscosinamide	$\text{CH}_3(\text{CH}_2)_6\text{CH}(\text{OH})\text{CH}_2\text{CO}$	L-Leu	D-Gln	D-aThr	D--Val	L-Leu	D-Ser	L-Leu	D-Ser	L-Ile
massetolide A	$\text{CH}_3(\text{CH}_2)_6\text{CH}(\text{OH})\text{CH}_2\text{CO}$	L-Leu	D-Glu	D-aThr	D-aIle	L-Leu	D-Ser	L-Leu	D-Ser	L-Ile
massetolide B	$\text{CH}_3(\text{CH}_2)_7\text{CH}(\text{OH})\text{CH}_2\text{CO}$	L-Leu	D-Glu	D-aThr	D-aIle	L-Leu	D-Ser	L-Leu	D-Ser	L-Ile
massetolide C	$\text{CH}_3(\text{CH}_2)_8\text{CH}(\text{OH})\text{CH}_2\text{CO}$	L-Leu	D-Glu	D-aThr	D-aIle	L-Leu	D-Ser	L-Leu	D-Ser	L-Ile
massetolide D	$\text{CH}_3(\text{CH}_2)_6\text{CH}(\text{OH})\text{CH}_2\text{CO}$	L-Leu	D-Gln	D-aThr	D-aIle	L-Leu	D-Ser	L-Leu	D-Ser	L-Leu
massetolide E	$\text{CH}_3(\text{CH}_2)_6\text{CH}(\text{OH})\text{CH}_2\text{CO}$	L-Leu	D-Glu	D-aThr	D--Val	L-Leu	D-Ser	L-Leu	D-Ser	L-Val
massetolide F	$\text{CH}_3(\text{CH}_2)_6\text{CH}(\text{OH})\text{CH}_2\text{CO}$	L-Leu	D-Glu	D-aThr	D--Val	L-Leu	D-Ser	L-Leu	D-Ser	L-Leu
massetolide G	$\text{CH}_3(\text{CH}_2)_7\text{CH}(\text{OH})\text{CH}_2\text{CO}$	L-Leu	D-Glu	D-aThr	D--Val	L-Leu	D-Ser	L-Leu	D-Ser	L-Ile
massetolide H	$\text{CH}_3(\text{CH}_2)_8\text{CH}(\text{OH})\text{CH}_2\text{CO}$	L-Leu	D-Glu	D-aThr	D--Val	L-Leu	D-Ser	L-Leu	D-Ser	L-Ile

Amphisin group

		1	2	3	4	5	6	7	8	9	10	11
amphisin	$\text{CH}_3(\text{CH}_2)_6\text{CH}(\text{OH})\text{CH}_2\text{CO}$	D-Leu	D-Asp	D-aThr	D--Leu	D-Leu	D-Ser	L-Leu	D-Gln	L-Leu	L-Ile	L-Asp
tensin	$\text{CH}_3(\text{CH}_2)_6\text{CH}(\text{OH})\text{CH}_2\text{CO}$	D-Leu	D-Asp	D-aThr	D--Leu	D-Leu	D-Ser	L-Leu	D-Gln	L-Leu	L-Ile	L-Glu

Figure 4. Overview of analogous CLPs to pseudodesmins A and B from both the viscosin and amphisin group. The conservation of the hydrophobic and hydrophilic residue positions can clearly be observed.

possibly be correlated with the opposite stereochemistry of the Leu5 residue. Viscosinamide has been found to be mainly active against plant pathogens such as *Rhizoctonia solani* and *Pythium ultimum*.^{4,13} While no antifungal activity for the pseudodesmins was observed, the pseudophomins have been found to be responsible for the antifungal activity of *P. fluorescens*.⁷ Because the latter compounds were not confronted against the same pathogens used here, a direct comparison can unfortunately not be made. WLIP was initially found to inhibit the brown blotch disease in *Agaricus bisporus* caused by *Pseudomonas tolaasi*¹⁵ and only later subjected to a more thorough biological screening against fungi and bacteria.¹² It was shown to display the same properties as the pseudodesmins in that it is mainly active against Gram positive but not against Gram negative bacteria. *Candida albicans*, *Cryptococcus neoformans* and *E. coli*, the only common pathogens in the WLIP and pseudodesmin screenings, were also found not to be inhibited by WLIP.

3.2. Conformation of pseudodesmin A and comparison to other CLPs

From the alignment of sequences in the viscosin group (Fig. 4), two subsets can be distinguished depending on whether Leu5 has an L (viscosin, viscosinamide and massetolides A–H) or D (WLIP, the pseudophomins and the pseudodesmins) configuration. This is motivated by the fact that other variations affect the nature of the side chains rather than the backbone. Since three dimensional structures have only been determined for the D-Leu type viscosin members, the structural impact of the D/L variation can unfortunately not yet be assessed. Given the high sequence similarity within the D-Leu subset, it is of no surprise that the crystal structure of pseudodesmin A is practically identical to those of WLIP¹⁶ and the pseudophomins.¹⁷ In all cases, the RMSD between the oligopeptide backbone and Thr3 side chain atom coordinates (29 atoms) is smaller than 0.03 Å. Consequently, the short α_L -helix present in pseudodesmin A is also present in these structures even though it was never recognized as such before. An NMR solution structure has been reported for WLIP as well,⁵ which was described to be significantly different from the crystal structure. Since the coordinates of this structure are not available, further comparisons cannot be made.

Helical structures in cyclic lipodepsipeptides have also been described outside the viscosin group. Amphisin¹⁸ and tensin¹⁹ (Fig. 4) are CLPs very similar to the viscosin group, but have a ring

structure built out of nine residues instead of seven. There are some substitutions of residues, but the overall pattern of hydrophobic and hydrophilic amino acids and D and L chirality is maintained. A crystal structure for both these CLPs has been reported and both possess an α_L -helix of equal number of residues to pseudodesmin A, while the extra residues are accommodated in the C-terminal loop. The RMSD of the backbone of this helix to the pseudodesmin A structure measured starting from the amide of residue 2 to the carbonyl of residue 5 (12 atoms) is only 0.15 Å for amphisin and 0.12 Å for tensin. Other CLPs are also described to contain α -helices, including tolaasin, fuscopeptin and syringopeptin.¹ It appears therefore that the α -helix is a common structure among many CLPs, suggesting a role of importance for their biological function.

An important feature of the pseudodesmin A structure is that it is amphipatic. Indeed, all hydrophobic and hydrophilic residues in the sequence occur at positions that arrange their side chains on opposite sides of the molecule (Fig. 5). This includes the three-residue loop region where the L–D–L stereochemistry allows the hydrophilic D-Ser8 side chain to be oriented towards the opposite side of the structure with respect to the hydrophobic L-Leu7 and L-Ile9 side chains. All together, this creates a large hydrophobic

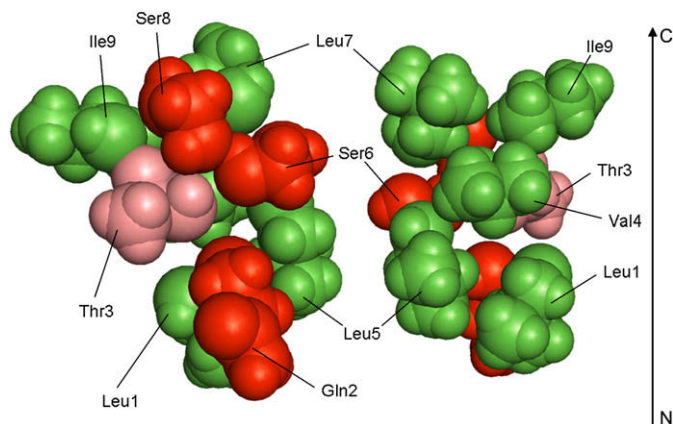


Figure 5. Sphere representation of the crystal structure of pseudodesmin A to illustrate the amphipaticity, showing only the side chain atoms starting from CH α . The hydrophobic and hydrophilic sides are shown separately, while the α -helix is aligned from bottom to top (N→C) as indicated by the arrow. Hydrophobic side chains are coloured green, hydrophilic side chains red and the Thr3 residue salmon. The HDA residue is left out for clarity.

surface, comprised of all Leu, Ile and Val side chains. A smaller hydrophilic surface includes both Ser residues and the Gln residue side chains. The conservation of hydrophobic and hydrophilic residues within the viscosin group and the helical part of amphisin and tensin (Fig. 4) suggests that this amphipaticity is maintained between the different compounds and that it plays an important role in their function.

It has been hypothesized that the biological function and antibiotic mechanism of CLPs is related to the formation of passive transport ion channels in the cellular membranes. These will seriously destabilize the microorganism's metabolism by disturbing the ion concentrations in the cytoplasm. Within the viscosin group this has been postulated for viscosinamide, which is believed to induce Ca^{2+} transporting pores to inhibit fungal growth.¹³ Furthermore, WLIP has been shown to insert itself within model membranes,²⁰ while its pore forming capability was demonstrated on erythrocytes using osmotic protectants.¹² The observed properties of pseudodesmin A are in agreement with such behaviour. The fact that the compound is practically water insoluble together with the high degree of hydrophobic side chains and the fatty acid moiety makes an insertion into the apolar membrane plausible. The amphipatic nature of the molecule suggests a model for pore formation that involves the formation of reverse type micelles inside the membrane. The molecules pack together with their hydrophilic surfaces towards each other while extending the hydrophobic surfaces outward to minimize the hydrophobic–hydrophilic contacts with the environment. Independent of the exact supramolecular structure that will be formed, these reverse micelles would be able to span the membrane, allowing ions to be transported through the hydrophilic pore created. This principle has been described previously, for instance for syringomycin.²¹

4. Experimental

4.1. Culture, isolation and purification of pseudodesmins A and B

The original *Pseudomonas tolaassii* strain was collected from the skin of a black belly salamander (*Desmognathus quadramaculatus*) and was a gift from R. Austin (Plethodon Research, L.L.C., 1590 Double Springs Road, Demorest, GA 30535, USA). Isolation, preliminary characterization and biological screening have been described previously.²²

Following fermentation of the bacterium using standard procedures, the fermentation broth was extracted with ethyl acetate, dried over MgSO_4 and concentrated in vacuo. The residue was redissolved in acetone and a first purification was done using a normal phase open column (Kieselgel 60, 230–400 mesh ASTM, Merck) with following eluents: hexane/acetone (8:2), hexane/acetone (1:1), acetone and ethanol. The fractions collected after eluting with acetone contained the bioactive material. After concentrating, the compound was brought on a preparative TLC (PLC) plate (Silicagel 60, 20×20 cm, 0.5 mm layer thickness, Merck) and eluted with dichloromethane/methanol (96:4). The fractions were scraped off and the molecules extracted from the silica with methanol. The band between R_f values 0 and 0.08 contained the antibacterial molecules. Preliminary LC–MS analysis of this fraction showed the strong presence of a molecule with protonated mass $[\text{M}+\text{H}]^+$ of 1125.3 Da. The LC–MS consisted of a Waters 2690 HPLC with Photodiode Array Detector (Waters 996) coupled to a Micromass Q-TOF 2 mass spectrometer. The column used was from Beckman (Ultrasphere; C-18; 5 μm , 150×4.6 mm) with guard column 7.5×4.6 mm, packed with the same material; eluent: acetonitrile/10 mM NH_4OAc in water with 0.1% TFA (60:40; flow: 1.5 ml/min); detection: 210 nm; retention time: 14.4 min (pseudodesmin A) or 11.1 min (pseudodesmin B),

measured from the UV chromatograms. MS spectra were taken in positive electrospray ionization mode with capillary voltage set at 2.5 kV, the cone voltage at 60 V, a collision energy of 15 eV, the microchannel plate at 2150 V, the source temperature at 100 °C and the desolvation temperature at 250 °C. The fragmentation of the parent ion ($\text{M}+\text{H}^+$) was studied via MS/MS analysis in positive electrospray ionization mode with a capillary voltage of 2 kV, the cone voltage at 60 V and the collision energy at 41 eV. The rest of the parameters was the same as mentioned above. For further analysis, both compounds, pseudodesmins A and B, were obtained in larger quantities as white solids, with yields of 260 mg and 27 mg, respectively, which corresponds to 0.163% and 0.0169% of weight compared to the collected freeze dried biological material. This is fully described in Supplementary data.

4.2. Biological screening

The screening for biological activity involved a selection of pathogens, including bacteria (*Enterococcus faecalis* ATCC 29212/LMG 8222, vancomycin resistant *Enterococcus* (VRE) ATCC 700221, *S. aureus* ATCC 29213/LMG 10147, methicillin resistant *S. aureus* (MRSA) ATCC 33591/LMG 16217, *Pseudomonas aeruginosa* ATCC 27853/LMG 6395, *Salmonella typhimurium* ATCC 700408/LMG 16217, *Clostridium perfringens* ATCC 13124, *E. coli* ATCC 25922), yeasts (*C. albicans* IHEM 10248 ATCC 24433 and *C. neoformans* IHEM 9558 ATCC 90112) and one mould (*Trichophyton mentagrophytes* IHEM 10342/ATCC 9533). *C. perfringens* was obtained from Oxoid as a Culti-Loop culture and grown in Anaerobe Basal broth (Oxoid, CM 957), while the other microorganisms were obtained from the Belgian Coordinated Collections of Microorganisms (BCCM).

All the bacteria were grown for 18 h in Mueller–Hinton broth (MHB, Oxoid, CM 405). Instant suspensions were prepared in 5 ml quantities of sterile saline. After standardization according to the 0.5 McFarland standard, the suspensions were further diluted to a final inoculum of approximately 5×10^5 CFU/ml.

For both the yeasts, a RPMI 1640 broth supplemented with 0.3 g/l glutamine and 34.6 g/l 3-(*N*-morpholino)propanesulfonic acid (MOPS-buffer) without bicarbonate was used. The yeasts were then sub-cultured at 35 °C onto Sabouraud dextrose agar and passaged twice to ensure purity and viability. Five colonies of ≥ 1 mm diameter from 24 h (*C. albicans*) or 48 h (*C. neoformans*) old cultures were picked and suspended in 5 ml of sterile 0.85% saline. The suspension cell densities were then standardized to a 0.5 McFarland standard with sterile saline by measuring the transmittance of a spectrophotometer at 530 nm. The obtained suspensions of $1\text{--}5 \times 10^6$ cells per ml were further diluted to obtain a final inoculum of $1\text{--}5 \times 10^3$ CFU/ml.

For the mould, a seven days old culture was covered with approximately 1 ml of sterile 0.85% saline. A suspension was made and one drop of Tween 20 was added. The resulting mixture of spores and hyphal fragments was transferred to a sterile tube and allowed to settle. The upper homogeneous suspension was collected and mixed. The densities of these spore suspensions were then adjusted to an optical density (OD) of 75% transmittance at 530 nm. The obtained suspension was further diluted in RPMI 1640 broth to obtain a final inoculum of 4×10^3 to 5×10^4 CFU/ml.

The minimum inhibitory concentration (MIC) was determined for both pseudodesmins on every pathogen next to a quality positive control compound,²³ being for the bacteria either vancomycin (Fluka/BioChemika 94747) or gentamycin (Fluka/Biochemika 48760) and for the yeasts and the mould amphotericin B (Fluka/Biochemika 10047); 2500 ppm solutions in DMSO were obtained of all test chemicals and further diluted 10-fold in a 11:1 demineralized water/DMSO mixture.

A robotic Bioscreen apparatus (Labsystems, Finland) operating under Biolink software was used, which measures the change in OD

(using white light, Wide Band) of the broth culture. Each of the 100 well honeycomb plates (Labsystems) contained 225 μ l MHB (RPMI 1640, 0.3 g/l glutamine and 34.6 g/l MOPS-buffer without bicarbonate for the mould) and 25 μ l of the solvent (negative control), test-chemical dilution, or positive control. The inoculum was added to the broth, except for the blank tests. The bacteria, *C. albicans*, *C. neoformans* and the mould were incubated for 16, 24, 48 h and 5 days, respectively, at 35 °C (25 °C for the mould), with every 20 min an OD measurement after medium shaking. *C. perfringens* was incubated under an anaerobic environment purged with CO₂.

Each test was repeated five times and the average was calculated. A blank test was performed with only the test chemical and MHB in the well and the difference Δ between the sample and blank areas was calculated. Negative control incubation tests were performed in an analogous manner except for the absence of test chemicals, resulting in an obtained value Δ_{NC} . The percent of growth was then calculated as $(\Delta/\Delta_{NC}) \times 100\%$, which was chosen as critical parameter for the evaluation of possible activity. For the mould, instead of kinetic measurements, the difference between final and initial OD values was used. Each test was repeated five times and the average was calculated.

In addition, the mixture of pseudodesmins A and B was screened for antiviral and antitumor effects at the Rega Institute (K.U. Leuven) against various pathogenic viruses such as human immunodeficiency virus (HIV), herpes simplex virus (HSV), vaccinia virus (VV), varicella zoster virus (VZV) and human cytomegalovirus (CMV). Antiviral activity was determined as the effective compound concentration (EC₅₀) required to inhibit by 50% HIV-induced cytopathicity in human CEM cell cultures, HSV- and VV-induced cytopathicity in human embryo fibroblast E₆SM cell cultures, VZV-induced plaque formation in human embryonic lung (HEL) cell cultures and as the concentration (IC₅₀) required to inhibit CMV-induced plaque formation by 50% using HEL cells. Antitumor activity was determined via the inhibitory effects on the proliferation of murine leukaemia cells (L1210/0), murine mammary carcinoma cells (FM3A/0) and human T-lymphocyte cells (Molt4/C8, CEM/0).

4.3. LC-MS analysis of the amino acid composition

For this analysis, 6.6 mg of pseudodesmin A was hydrolyzed by dissolving it in 6.6 ml 6 M HCl together with 136 mg phenol for 20 h at 110 °C. After solvent evaporation in vacuo, the residue was dissolved in 5.28 ml of H₂O and 2.29 ml of a 3.7 mM solution of Marfey's reagent¹⁴ in acetone to which 528 μ l of 1 M NaHCO₃ were added to derivatize the free amino acids formed. After stirring this mixture for 1 h at 40 °C, 264 μ l of a 2 M HCl solution was added and the solvent was evaporated. The residue was dissolved in 8.8 ml DMSO and 60 μ l of this solution was diluted to 200 μ l with a 40:60 mixture of acetonitrile/NH₄OAc 5 mM. Standard solutions of L- and D-amino acids derivatized with Marfey's reagent were prepared by adding 50 μ l 50 mM amino acid aqueous solution to 100 μ l of 3.7 mM Marfey's reagent in acetone and 20 μ l of 1 M NaHCO₃. After 1 h at 40 °C, 10 μ l of 2 M HCl was added, the solvent was removed in vacuo and the residue was dissolved in 500 μ l DMSO. This was done separately for several amino acids. By taking 30 μ l of every solution, the following mixtures were made and diluted to 200 μ l with a 40:60 mixture of acetonitrile/NH₄OAc 5 mM: D-Leu+D-Val+D-Thr, L-Leu+L-Val+L-Thr, D-Ile+D-Ser, L-Ile+L-Ser, D-Glu, L-Glu, D-allo-Thr, L-allo-Thr. All samples were injected on an HPLC column (Ultrasphere C18 5 μ m, 150 \times 4.6 mm I.D., fitted with a precolumn with the same stationary phase, 7.5 \times 4.6 mm I.D.) hyphenated to a UV-detector operating at a wavelength of 350 nm for peak integration and a Q-TOF mass spectrometer using negative mode electrospray as ionization technique. The mobile phase, acetonitrile/NH₄OAc

5 mM, was linearly changed from a 10:90 to 28:72 mixture over a time span of 36 min.

4.4. NMR spectroscopy

All NMR measurements were performed on either a Bruker DRX spectrometer operating at 500.13 MHz and 125.76 MHz for the ¹H and ¹³C frequency, respectively, or a Bruker Avance II spectrometer operating at 700.13 MHz, 176.05 MHz and 70.94 MHz for ¹H, ¹³C and ¹⁵N, respectively. In both cases, a ¹H, ¹³C, ¹⁵N TXI-Z probe was used. The sample temperature was set to 298.0 K. High quality NE-HP5-7 (New Era Ent. Inc) NMR tubes were used. Acetonitrile-*d*₃ (99.96%) was purchased from Eurisotop, 2D spectra measured for structure elucidation include gradient selected phase sensitive DQF-COSY, TOCSY with a 90 ms MLEV-17 spinlock, NOESY with mixing times ranging between 100 ms and 300 ms, gradient selected ¹H-¹³C gHSQC and ¹H-¹⁵N gHSQC and gradient selected ¹H-¹³C gHMBC. Standard pulse sequences as present in the Bruker library were used throughout.²⁴ Typically, 4096 data points were sampled in the direct dimension for 512 data points in the indirect dimension, with the spectral width, respectively, set to 11 ppm, 170 ppm and 80 ppm along the ¹H, ¹³C and ¹⁵N dimension. The ¹H-¹³C gHMBC was measured with an 88 ppm ¹³C spectral width centred on the carbonyl chemical shift region. For 2D processing, the spectra were zero filled until a 4096 \times 2048 real data matrix. Before Fourier transformation, all spectra were multiplied with a squared cosine bell function in both dimensions or sine bell in the direct dimension for the gHMBC. The ¹H and ¹³C chemical shifts are referenced against internal TMS, while the ¹⁵N chemical shift was referenced indirectly to MeNO₂ according to IUPAC guidelines.²⁵ Scalar couplings were obtained from the Gaussian resolution enhanced 1D ¹H spectrum.

4.5. Crystal growth and X-ray structure determination

Following extensive screening, colourless needle-like crystals of pseudodesmin A of sufficient quality for X-ray diffraction studies were finally obtained by slow evaporation from a concentrated solution in acetonitrile. X-ray data were collected on an Oxford Diffraction Gemini R Ultra diffractometer using monochromatic Cu K α radiation. The data were processed using the CrysAlis package (Oxford Diffraction (2007) CrysAlis CCD and CrysAlis RED, versions 1.171.32.5, Oxford Diffraction Ltd, Abingdon, Oxfordshire, England). The structure was solved with Sir92²⁶ and refined against low temperature data using full-matrix least-squares refinement within SHELXL97^{27,28} as available in the PLATON suite.²⁹ All H atoms were calculated geometrically and restrained to ride on their parent atoms. A correction for diffuse effects due to the inclusion of disordered solvent molecules in the crystal structure was made using the SQUEEZE option of PLATON. The total potential solvent volume per unit cell was calculated to be 261 Å³ (4% of the cell volume).

Acknowledgements

The Fund for Scientific Research—Flanders (FWO-Vlaanderen) is gratefully acknowledged for a Ph.D. fellowship to D.S. and various equipment grants (G.0365.03, G.0064.07) to J.C.M. C.M. thanks the Belgian National Fund for Scientific Research for her postdoctoral researcher position. The 700 MHz equipment of the Interuniversity NMR Facility was financed by Ghent University, the Free University of Brussels (VUB) and the University of Antwerp via the 'Zware Apparatuur' Incentive of the Flemish Government. This research is supported by the NMR Scientific Research Community of the FWO. Prof. Dr. Pat Sandra and Dr. Alberto dos Santos Pereira of the RIC are most gratefully thanked

for the high resolution mass spectrometry analysis. Dr. Rick Austin (Plethodon Inc) is gratefully acknowledged for the gift of a sample of *P. tolaasii*.

Supplementary data

Supplementary data associated with this article can be found in the online version, at doi:10.1016/j.tet.2009.03.045.

References and notes

1. Nybroe, O.; Sorensen, J. In *Pseudomonas Volume III—Macromolecules*; Ramos, J. L., Ed.; Kluwer Academic/Plenum: New York, NY, 2004; pp 147–172.
2. Raaijmakers, J. M.; de Bruijn, I.; de Kock, M. J. D. *Mol. Plant-Microbe Interact.* **2006**, *19*, 699–710.
3. Hiramoto, M.; Okada, K.; Nagai, S. *Tetrahedron Lett.* **1970**, 1087–1090.
4. Nielsen, T. H.; Christophersen, C.; Anthoni, U.; Sorensen, J. *J. Appl. Microbiol.* **1999**, *87*, 80–90.
5. Mortishire-Smith, R. J.; Nutkins, J. C.; Packman, L. C.; Brodey, C. L.; Rainey, P. B.; Johnstone, K.; Williams, D. H. *Tetrahedron* **1991**, *47*, 3645–3654.
6. Gerard, J.; Lloyd, R.; Barsby, T.; Haden, P.; Kelly, M. T.; Andersen, R. J. *J. Nat. Prod.* **1997**, *60*, 223–229.
7. Pedras, M. S. C.; Ismail, N.; Quail, J. W.; Boyetchko, S. M. *Phytochemistry* **2003**, *62*, 1105–1114.
8. Kochi, M.; Weiss, D. W.; Pugh, L. H.; Groupé, V. *Bacteriol. Proc.* **1951**, *1*, 29–30.
9. Saini, H. S.; Barragan-Huerta, B. E.; Lebron-Paler, A.; Pemberton, J. E.; Vazquez, R. R.; Burns, A. M.; Marron, M. T.; Seliga, C. J.; Gunatilaka, A. A. L.; Maier, R. M. *J. Nat. Prod.* **2008**, *71*, 1011–1015.
10. Laycock, M. V.; Hildebrand, P. D.; Thibault, P.; Walter, J. A.; Wright, J. L. C. *J. Agric. Food Chem.* **1991**, *39*, 483–489.
11. de Souza, J. T.; de Boer, M.; de Waard, P.; van Beek, T. A.; Raaijmakers, J. M. *Appl. Environ. Microbiol.* **2003**, *69*, 7161–7172.
12. Lo Cantore, P.; Lazzaroni, S.; Coraiola, M.; Dalla Serra, M.; Cafarchia, C.; Evidente, A.; Iacobellis, N. S. *Mol. Plant-Microbe Interact.* **2006**, *19*, 1113–1120.
13. Thrane, C.; Olsson, S.; Nielsen, T. H.; Sorensen, J. *FEMS Microbiol. Ecol.* **1999**, *30*, 11–23.
14. Marfey, P. *Carlsberg Res. Commun.* **1984**, *49*, 591–596.
15. Soler-Rivas, C.; Arpin, N.; Olivier, J. M.; Wichers, H. J. *J. Appl. Microbiol.* **1999**, *86*, 635–641.
16. Han, F. S.; Mortishire-Smith, R. J.; Rainey, P. B.; Williams, D. H. *Acta Crystallogr., Sect. C: Cryst. Struct. Commun.* **1992**, *48*, 1965–1968.
17. Quail, J. W.; Ismail, N.; Pedras, M. S. C.; Boyetchko, S. M. *Acta Crystallogr., Sect. C: Cryst. Struct. Commun.* **2002**, *58*, o268–o271.
18. Sorensen, D.; Nielsen, T. H.; Christophersen, C.; Sorensen, J.; Gajhede, M. *Acta Crystallogr., Sect. C: Cryst. Struct. Commun.* **2001**, *57*, 1123–1124.
19. Henriksen, A.; Anthoni, U.; Nielsen, T. H.; Sorensen, J.; Christophersen, C.; Gajhede, M. *Acta Crystallogr., Sect. C: Cryst. Struct. Commun.* **2000**, *56*, 113–115.
20. Coraiola, M.; Lo Cantore, P.; Lazzaroni, S.; Evidente, A.; Iacobellis, N. S.; Dalla Serra, M. *Biochim. Biophys. Acta, Biomembr.* **2006**, *1758*, 1713–1722.
21. Hutchison, M. L.; Tester, M. A.; Gross, D. C. *Mol. Plant-Microbe Interact.* **1995**, *8*, 610–620.
22. Austin, R. M., Jr.; Van Hemel, J.; Sas, B.; Vanderkerckhove, J. Patent application (Publication number WO/2002/078720, 2002, to be found at <http://www.wipo.int>).
23. National Committee for Clinical Laboratory Standards. *Methods for Dilution Antimicrobial Susceptibility Tests for Bacteria that Grow Aerobically*, 4th ed.; NCCLS: Wayne, PA, USA, 1997; Approved Standard M7-A4.
24. Berger, S.; Braun, S. *200 and More NMR Experiments: A practical Course*, 3rd ed.; John Wiley and Sons: Weinheim, 2004.
25. Harris, R. K.; Becker, E. D.; De Menezes, S. M. C.; Goodfellow, R.; Granger, P. *Pure Appl. Chem.* **2001**, *73*, 1795–1818.
26. Altomare, A.; Cascarano, G.; Giacobozzo, C.; Guagliardi, A. *J. Appl. Crystallogr.* **1993**, *26*, 343–350.
27. Sheldrick, G. *Acta Crystallogr., Sect. A: Found. Crystallogr.* **1984**, *40* C440–C440.
28. Vandersluis, P.; Spek, A. L. *Acta Crystallogr., Sect. A: Found. Crystallogr.* **1990**, *46*, 194–201.
29. Spek, A. L. *J. Appl. Crystallogr.* **2003**, *36*, 7–13.